Clinical Neurophysiology 128 (2017) 667–680

Contents lists available at ScienceDirect

Clinical Neurophysiology

journal homepage: www.elsevier.com/locate/clinph

# Functional and effective brain connectivity for discrimination between Alzheimer's patients and healthy individuals: A study on resting state EEG rhythms

Katarzyna J. Blinowska [a,b,*], Franciszek Rakowski [c,d], Maciej Kaminski [a], Fabrizio De Vico Fallani [e,f], Claudio Del Percio [g], Roberta Lizio [h,i], Claudio Babiloni [h,i]

[a] Faculty of Physics, Department of Biomedical Physics, University of Warsaw, Warsaw, Poland
[b] Nalecz Institute of Biocybernetics and Biomedical Engineering, Polish Academy of Sciences, Warsaw, Poland
[c] Interdisciplinary Centre for Mathematical and Computational Modelling, University of Warsaw, Poland
[d] Mossakowski Medical Research Centre, Polish Academy of Sciences, Warsaw, Poland
[e] Inria Paris, Aramis Project-team, 75013 Paris, France
[f] Sorbonne Universités, UPMC Univ Paris 06, Inserm, CNRS, Institut du cerveau et la moelle (ICM) – Hôpital Pitié-Salpêtrière, 75013 Paris, France
[g] Department of Integrated Imaging, IRCCS SDN, Napoli, Italy
[h] IRCCS San Raffaele Pisana, Rome, Italy
[i] Department of Physiology and Pharmacology, University of Rome "La Sapienza", Rome, Italy

See Editorial, pages 658–659

ARTICLE INFO

*Article history:*
Accepted 1 October 2016
Available online 22 October 2016

*Keywords:*
Alzheimer's disease
EEG rhythms
Granger causality
Directed transfer function (DTF)
Effective connectivity
Classification accuracy
Receiver operating characteristic (ROC)

## HIGHLIGHTS

- New multivariate EEG connectivity markers were tested on Alzheimerian's.
- Alzheimer's group showed decreased posterior-to-anterior EEG connectivity.
- Promising results of classification between AD and control group: AUC = 86%.

## ABSTRACT

*Objective:* This exploratory study provided a proof of concept of a new procedure using multivariate electroencephalographic (EEG) topographic markers of cortical connectivity to discriminate normal elderly (Nold) and Alzheimer's disease (AD) individuals.
*Method:* The new procedure was tested on an existing database formed by resting state eyes-closed EEG data (19 exploring electrodes of 10–20 system referenced to linked-ear reference electrodes) recorded in 42 AD patients with dementia (age: 65.9 years ± 8.5 standard deviation, SD) and 42 Nold non-consanguineous caregivers (age: 70.6 years ± 8.5 SD). In this procedure, spectral EEG coherence estimated reciprocal functional connectivity while non-normalized directed transfer function (NDTF) estimated effective connectivity. Principal component analysis and computation of Mahalanobis distance integrated and combined these EEG topographic markers of cortical connectivity. The area under receiver operating curve (AUC) indexed the classification accuracy.

*Abbreviations:* ACC, accuracy; AD, Alzheimer disease; ANN, artificial neural network; AUC, area under receiver operating curve; COH, matrix of coherence values; coh, outcome of the PCA upon the COH, feature used for classification; CSF, cerebro-spinal fluid; EEG, electroencephalogram; dDTF, direct directed transfer function; DTF, directed transfer function; DTI, diffusion tensor imaging; FDG, fluorodeoxyglucose; FFT, fast Fourier transform; ffDTF, full frequency directed transfer function; ffDTFp, outcome of the PCA upon the ffDTFpairs matrix, feature used for classification; ffDTFpairs, matrix of ffDTF values computed between all electrodes; FPR, false positive rate; IAF, individual alpha frequency (peak); MCI, mild cognitive impairment; MMSE, mini mental state examination; MRI, magnetic resonance imaging; MVAR, multivariate autoregressive model; NDTF, non normalized directed transfer function; NDTFpairs, matrix of NDTF values computed between all electrodes; NDTFp, outcome of the PCA upon the NDTFpairs matrix, feature used for classification; NDTFsource, NDTF values computed between a given electrode and all the remaining ones; NDTFs, outcome of the PCA upon the NDTFsource, feature used for classification; NDTFs(c), parameter characterizing decay of NDTF with the distance; Nold, old healthy people (group); PET, positron emission tomography; PC, principal component; PC1, first principal component; PC2, second principal component; PCA, principal component analysis; ROC, receiver operating curve; SEN, sensitivity; SES, stochastic event synchrony; SPE, specificity; SPECT, single photon emission computer tomography; TPR, true positive rate.

* Corresponding author at: Department of Biomedical Physics, Faculty of Physics, University of Warsaw, Pasteura 5, 02-093 Warszawa, Poland. Fax: +48 22 659 1030.
*E-mail address:* kjbli@fuw.edu.pl (K.J. Blinowska).

http://dx.doi.org/10.1016/j.clinph.2016.10.002

*Results:* A good classification of Nold and AD individuals was obtained by combining the EEG markers derived from NDTF and coherence (AUC = 86%, sensitivity = 0.85, specificity = 0.70).
*Conclusion:* These encouraging results motivate a cross-validation study of the new procedure in age- and education-matched Nold, stable and progressing mild cognitive impairment individuals, and de novo AD patients with dementia.
*Significance:* If cross-validated, the new procedure will provide cheap, broadly available, repeatable over time, and entirely non-invasive EEG topographic markers reflecting abnormal cortical connectivity in AD patients diagnosed by direct or indirect measurement of cerebral amyloid β and hyperphosphorylated tau peptides.


## 1. Introduction

Among many causes of dementia, the most common in geriatric patients is Alzheimer's disease (AD). AD is characterized by a pathological brain accumulation of amyloid β and hyperphosphorylated tau peptides inducing neurodegeneration and decrease of cholinergic tone (Terry and Buccafusco, 2003). In recent guidelines concerning AD (Dubois et al., 2014), amyloid β and tau proteins in cerebrospinal fluid (CSF) and positron emission tomography (PET) maps of amyloid β and tau in the brain were proposed as *pathophysiological markers* for an early biological diagnosis of AD, while magnetic resonance imaging (MRI) and FDG-PET procedures were proposed as *topographic markers* to track a disease evolution by indexes of brain structural integrity and metabolism, respectively. However, the above CSF and neuroimaging biomarkers derive from procedures that are not widely available in the clinical environment, expensive, and partly invasive. These reasons motivate the quest for integrative or alternative biomarkers for early diagnosis, disease tracking, and therapy monitoring of AD. A promising cheap, largely available, repeatable over time without learning effects, and entirely non-invasive neurophysiologic technique is the recording of electroencephalographic (EEG) rhythms in the condition of awake resting state eyes-closed In the last years, there was an increasing interest in the analysis of these EEG rhythms, as a promising methodology for the development of a non-invasive, cheap, and repeatable topographic markers for a neurophysiological assessment of AD patients useful for clinical decision making along the progression of the disease (Anderer et al., 1994; Lehmann et al., 2007; Jackson and Snyder, 2008; Rossini et al., 2007, 2008; Babiloni et al., 2013). This neurophysiological assessment may enrich the clinical evaluation even if it has not the feature of a diagnostic procedure based on the direct or indirect measurement of amyloid β and hyperphosphorylated tau peptides.

In the review paper by Jeong (2004), the following hallmarks of EEG abnormalities in AD patients were reported: shift of the EEG power spectrum to lower frequencies, less complex EEG activity, and decrease in coherence of fast EEG rhythms. In the literature, the general accuracy of the classification of individual mild AD patients by spectral EEG markers has been estimated at around 80% (Claus et al., 1999; Huang et al., 2000; Bennys et al., 2001; Buscema et al., 2007).

In a more recent review by Dauwels et al. (2010a), similar major effects of AD on EEG rhythms were reported: slowing of EEG, reduced complexity of EEG signals, and perturbations in EEG synchrony. In that review, measures quantifying the above mentioned effects were described, several state-of-the-art pre-processing techniques were outlined, and limitations of computational approaches for diagnosing AD based on EEG were discussed.

It has been recently suggested that AD amyloidosis and neurodegeneration typically affect distributed brain neuronal networks subserving cognitive functions (Pievani et al., 2011; Braak et al., 2006) and induce a functional brain disconnection syndrome (Delbeuck et al., 2003). In this context, investigation of brain connectivity seems a promising method to provide additional biomarkers of AD pathology. The concept of "functional brain connectivity" refers to the interaction between two or more neural systems, either at a synaptic or population level, which is reflected by a statistical dependence of a variable describing the activation or deactivation of those systems (Friston, 2011). Functional brain connectivity does not imply the existence of anatomical connection or causal influence of one system on another. It can be typically indexed by measures such as statistical correlation (in the time domain) and spectral coherence (in the frequency domain). There is an important limitation of the functional connectivity computed from EEG signals recorded at different scalp regions. It may depend not only on neural currents of the underlying cortical region but also on neural currents generated by remote cortical regions and conducted across head volume (the so-called "volume conduction"). Furthermore, two cortical regions can show correlated activations because of "common feeding" from a third cortical or sub-cortical source.

Effective connectivity is another important dimension of functional connectivity, which refers to a causal influence that one neural system exerts on another and can be estimated by measures based on Granger causality (Kaminski et al., 2001; Blinowska and Zygierewicz, 2012). A convenient measure of effective brain connectivity is directed transfer function (DTF): (Kaminski and Blinowska, 1991). DTF alleviates the effects of "common feeding" and volume conduction (Kaminski and Blinowska, 2014).

A bulk of previous EEG studies has shown an abnormal spectral coherence and DTF connectivity in AD subjects at the group level. On one hand, the spectral coherence of EEG rhythms differed between healthy elderly (Nold) and AD subjects. Namely, the majority of previous EEG studies have reported a prominent decrease of the spectral coherence, especially at the alpha band, in the AD in respect to Nold subjects (for a review see Babiloni et al., 2015). On the other hand, DTF values have unveiled a reduction in the parietal-to-frontal inter-relatedness of delta and alpha rhythms in AD and mild cognitive impairment (MCI) patients in comparison to Nold subjects (Babiloni et al., 2008; Babiloni et al., 2009a,b; Blinowska et al., 2012).

A recent seminal EEG study (Dauwels et al., 2010b) compared the classification accuracy of data from MCI patients that later suffered from AD versus data of Nold subjects by: partial directed coherence, DTF, full frequency DTF (ffDTF), state space based estimators, different kinds of entropy measures, different kinds of divergence and stochastic event synchrony (SES), and information-theoretic measures including Mutual Information (measure closely related to Synchronization Likelihood). Results showed that the majority of these EEG estimates globally indicated a decrease of the functional and effective brain connectivity in AD

patients with respect to Nold subjects, however only two estimators yielded significant results in the classification of Nold and MCI individuals, namely SES (sensitivity = 68,35%) and ffDTF – full frequency DTF (sensitivity = 70.0%).

Different synchrony measures (coherences, DTF, ffDTF, dDTF, omega complexity[1]) were also used in a hybrid approach (Gallego-Jutgla et al., 2015), concerning early Alzheimer disease diagnosis, where relative power in different frequency bands was considered as well. It was demonstrated that combining parameters describing EEG slowing and changes in EEG synchrony gives very good classification results and improves the ability to distinguish between AD patients and healthy subjects. However, as the Authors admitted themselves, further studies on the larger database are needed to generalize the results.

Keeping in mind the above results and considerations, the present exploratory study tested the hypothesis that multivariate spectral coherence and DTF topographic markers provide a good discrimination between Nold and AD subjects, when the classification of resting state EEG rhythms is performed on features obtained by preliminary procedures extracting and integrating main information contents of the above estimators (e.g. Principal component analysis, PCA; computation of Mahalanobis distance; for more details see Section 2). A correct classification of these Nold and AD subjects would provide a first proof of concept that those EEG topographic markers unveil abnormal neurophysiological mechanisms generating the propagation of EEG signals in the cerebral cortex, even if they are not specific for AD and cannot be considered as "diagnostic" (they do not measure primary disease pathophysiological markers directly).

To this aim, the new procedure of this study was applied on an available clinical and EEG database in Nold subjects and AD patients with dementia. The database had two convenient features. The Nold and AD individuals had a paired socio-economic factor basically, and EEG data were recorded from them using an extracephalic reference electrode. This methodological feature made the recorded EEG data compatible with advanced multivariate techniques for the extraction of markers of functional and effective EEG connectivity.

Aside these favorable aspects, the mentioned database had some methodological limitations. The present groups of Nold and AD subjects were relatively small and not perfectly matched in respect of age and education. Furthermore, all AD patients assumed psychoactive medications typically administered in this disease (i.e. Acetylcholinesterase inhibitors). Finally, the database lacked control groups of MCI seniors stable across time or patients with dementia due to non-AD etiologies. Nevertheless, the current exploratory study globally provided a first proof of concept on the classification accuracy of the new step-wise procedure in Nold and AD individuals.

## 2. Material and methods

### 2.1. Subjects and diagnostic criteria

EEG signals of the present study were available in the archive of European FP7 project DECIDE (http://eu-decide.eu). This EEG archive was formed by a past multicenter investigation enrolling all consecutive AD patients with dementia and non-consanguineous family caregivers and strict friends (no consanguineous relative was included) to minimize differences in socio-economic and environmental factors. Those factors include financial resources, access to medical care, quality of the life, features of the house and city/town, which might affect global personal wellness, brain function, and EEG activity. Noteworthy, the composition of that EEG database reflected the AD population and that of their caregivers. Indeed, AD patients are typically older and less educated than their non-consanguineous family caregivers are. Another feature of the mentioned EEG archive concerns the reference electrode. In neurologic and geriatric departments, clinical EEG recordings are often performed using a cephalic reference electrode incorporated into an elastic electrode cap, which allows sparing the time to apply extracephalic reference electrodes on linked ears, mastoids or nose.

In the present study, we used the part of the DECIDE EEG database comprising all individual EEG datasets recorded with an extracephalic electrode reference (i.e. "linked ears"). The reason is that only EEG recordings with extracephalic electrode references are adequate for mathematical approaches based on autoregressive models using the phase of the EEG rhythms to model the functional or effective connectivity between electrode pairs. As another constraint, we used the part of the DECIDE EEG database having a full clinical documentation that minimized the risk of a diagnostic misclassification with other kinds of dementing disorders (i.e. cerebrovascular dementia, frontotemporal dementia, dementia of Lewy body, etc.). As a result, we formed relatively small groups of AD and Nold individuals reflecting the typical epidemiological characteristics of AD population and that of their caregivers.

Keeping in mind the above considerations and constraints, the present study was based on clinical and EEG datasets of 42 Nold subjects and 42 AD patients with mild to moderate dementia. Table 1 reports relevant demographic and clinical information on both groups. For the reasons explained above, these groups showed some difference as age (about 5 years, on average) and education (the AD patients were older and less educated than the Nold subjects were). Because of the present methodological approach is grounded on statistical procedures requiring relatively large databases (i.e. principal component analysis), we did not remove many Nold and AD individuals to pair age and education in the two groups.

Probable ADD was diagnosed according to the criteria of the Diagnostic and Statistical Manual of Mental Disorders, fourth edition (DSM-IV-TR) (American Psychiatric Association. Diagnostic and statistical manual of mental disorders (IV-TR), 4th edn—text revised. Washington, DC; 2000) and the National Institute of Neurological Disorders and Stroke–Alzheimer Disease and Related Disorders (NINCDS–ADRDA) working group (McKhann et al., 1984).

Probable AD was diagnosed according to the criteria of the DSM-IV-TR (American Psychiatric Association. Diagnostic and statistical manual of mental disorders (IV-TR), 4th edn—text revised. Washington, DC; 2000) and the NINCDS-ADRDA (McKhann et al., 1984). The mild AD patients underwent general medical, psychiatric, and neurological assessments. They were also rated on some standardized clinical scales that included MMSE (Folstein et al., 1975), geriatric depression scale (GDS; Yesavage et al., 1982), clinical deterioration rate (CDR; Hughes et al., 1982), Instrumental Activities of Daily Living scale (IADL, Lawton and Brodie, 1969), and Hachinski Ischemic Score (HIS, Rosen et al., 1980). Complete laboratory analyses and neuroimaging diagnostic procedures (MRI) were carried out to exclude other causes of progressive or reversible dementias, to have a clinically homogenous mild AD patient group. Inclusion criteria were as follows: (i) objective impairment on neuropsychological evaluation—as defined by performances under the mean value of 1.5 standard deviations (SD) or greater for age- and education-matched controls for a neuropsychological test battery, to assess cognitive performance in the domains of language, memory (i.e., Busckhe-Fuld and Memory

[1] dDTF—direct DTF is based on combination of partial coherences and DTF, omega complexity-synchrony is evaluated with principal component analysis of the obtained covariance of data.

**Table 1**
Demographic and clinical data of the data-set of 42 healthy elderly (Nold), and 42 Alzheimer (AD) subjects used in the study. (MMSE – Mini Mental State Examination score – Folstein et al.,1983; IAF – Individual Alpha Frequency Peak).

| | Subjects (N) | Gender (M/F) | Age (years) | Education (years) | MMSE (score) | IAF (Hz) |
|---|---|---|---|---|---|---|
| Nold | 42 | 21/21 | 65.9 (±8.5 SD) | 12.0 (±4.6 SD) | 28.8 (±1.5 SD) | 10.6 (±2.6 SD) |
| AD | 42 | 14/28 | 70.6 (±8.5 SD) | 6.3 (±3.0 SD) | 19.3 (±5.2 SD) | 9.0 (±1.3 SD) |

Rey tests), visuoconstruction, and executive function/attention (ii) CDR score higher than 0.5 and (iii) abnormal activities of daily living as attested by the history and evidence of independent living.

Exclusion criteria included, especially, any evidence of (i) Lewy body dementia, (ii) vascular dementia, diagnosed according to NINDS-AIREN criteria (Roman et al., 1993), (iii) frontotemporal dementia, diagnosed according to criteria of Lund and Manchester Groups (1994), (iv) reversible dementias (including pseudodementia of depression); and (v) extrapyramidal syndromes. When given, antidepressant and/or antihypertensive, and benzodiazepines were suspended for about 24 h before EEG recordings. This did not provide a complete washout of the drug –longer periods would not have been applicable for obvious ethical reasons- but it made possible to compare the drug condition across the patients.

The AD patients of the present study suffered from a mild to moderate stage of dementia. They all followed a long-term treatment with standard daily doses of acetylcholinesterase inhibitors such as donepezil (23 patients; 5–10 mg/die), rivastigmine (12 patients; 10 mg/die) or galantamine (7 patients; 16–36 mg/die). A minority of these patients (less than 15%) used anxiolytic benzodiazepine or antidepressant agents to mitigate non-cognitive symptoms. According to the clinical practice, the AD patients were asked to take their medication immediately after the EEG recording performed in the morning. This procedure induced neither a discontinuation syndrome nor a complete washout of the drug but paired the period from the last assumption of the drugs and EEG recording across the AD subjects.

A battery of neuropsychological tests assessed general cognitive performance in the domains of language, memory, visuoconstruction, and executive function/attention abilities.

The tests assessing memory included the delayed recall of Rey figures (Rey, 1968), and/or the delayed recall of a story (Spinnler and Tognoni, 1987). The tests assessing language included the 1-minute verbal fluency for letters, fruits, animals or car trades (Novelli et al., 1986), and/or the Token test (Spinnler and Tognoni, 1987). The tests assessing executive function and attention included the Trail Making Test part A and B (Reitan, 1958). Finally, the tests assessing visuoconstruction included the copy of Rey figures.

The Nold subjects were recruited mainly among non-consanguineous relatives of AD patients. All Nold subjects underwent cognitive screening (including MMSE and GDS) as well as physical and neurological examinations to exclude any type of dementia. Subjects affected by chronic systemic illnesses (e.g. diabetes mellitus) were excluded, as well as subjects receiving psychoactive drugs. Subjects with a history of previous or present psychiatric or neurological disease were also excluded. All Nold subjects had a GDS score lower than 14 (no depression).

### 2.2. EEG data recording and preliminary EEG data analysis

EEG recordings were performed at resting state eyes closed. As a general clinical practice, all individuals had been preliminarily instructed not to take substances, foods, and drinks with nicotine, caffeine, theine, alcohol, and other stimulants in the morning of the EEG experiment. Furthermore, the subjects' general use of these psychoactive agents were preliminarily checked before the EEG recordings. The EEG signals were recorded from 19 scalp electrodes positioned according to the 10–20 system, using "linked ears" as a reference electrode, which is the standard in the clinical application of neurophysiology. The EEG signals were filtered in the band-pass 0.4–45 Hz range in a way preserving EEG phases and sampled at 128 Hz or 256 Hz. Those sampled at 256 Hz were down-sampled to 128 Hz.

The EEG data (128 Hz) were analyzed and segmented off-line in consecutive epochs of 2 s. The EEG epochs with muscular, ocular, and other types of artifact were preliminarily identified by an automatic computerized procedure. Two independent experimenters blind to the diagnosis visually confirmed the EEG segments accepted for further analysis. Of note, particular attention was devoted to avoiding an inclusion of EEG segments and individual data sets with EEG signs of drowsiness or pre-sleep stages.

### 2.3. Computation of EEG power density and IAF peak

A digital FFT-based power spectrum analysis (Welch method, Hanning windowing function, no phase shift) computed power density of the EEG rhythms with 0.5 Hz frequency resolution. The computation of EEG power density allowed the identification of IAF peak, that is the frequency associated with the maximum power density peak at the extended alpha range of 7–14 Hz (Klimesch, 1999).

### 2.4. Estimation of directed transfer function (DTF)

Calculation of connectivity estimators was performed in the framework of Multivariate Autoregressive Model. Ordinary, partial and multiple coherences and directed transfer function were estimated (Blinowska and Kaminski, 2006). The DTF (Kaminski and Blinowska, 1991) is an estimator of effective connectivity, based on MVAR. It may be considered as an extension of the Granger causality principle (Granger, 1967) to the arbitrary number of channels (Kaminski et al., 2001). DTF estimates a causal influence of EEG channel $j$ on channel $i$ at frequency $f$:

$$\mathrm{DTF}_{j\to i}(f) = \frac{|H_{ij}(f)|^2}{\sum_{m=1}^{k}|H_{im}(f)|^2} \tag{1}$$

where $H_{im}$ is the transfer function of the MVAR model. The formula describes the propagation from the EEG channel $j$ to $i$ in respect to inflows to the destination EEG channel $i$ from other channels. In the above formula, the denominator is dependent on frequency, so the spectral characteristics of DTF depend on the frequency properties of all EEG channels, but not only EEG input channel. To avoid this influence, the ffDTF function was introduced. In ffDTF, the denominator is integrated over frequencies, in this way the spectrum of the estimator ffDTF is not influenced by the frequency characteristics of the denominator

$$\mathrm{ffDTF}_{j\to i}(f) = \frac{|H_{ij}(f)|^2}{\sum_f\sum_{m=1}^{k}|H_{im}(f)|^2} \tag{2}$$

DTF and ffDTF are normalized in such a way that they take values from 0 to 1. If we are interested in the absolute strengths of transmissions between EEG channels we can abandon the normalization factor and introduce Non-normalized DTF—NDTF:

$$\mathrm{NDTF}_{j\to i}(f) = |H_{ij}(f)|^2 \quad (3)$$

It was demonstrated by modeling studies (Kaminski et al., 2001), that NDTF is proportional to the causal coupling between the EEG channels $j$ and $i$. Therefore, NDTF is a measure of effective connectivity. Coherence is a measure of functional connectivity. However, it does not imply a causal connection between time series.

The detailed description of the estimation of the MVAR and DTF can be found in previous studies (Blinowska and Kaminski, 2006; Blinowska and Zygierewicz, 2012). In those studies, properties of DTF, some of its applications, and comparison with other measures of EEG functional connectivity are reported. On the whole, it has been demonstrated that DTF and its modifications are robust with respect to noise and head volume conduction. Indeed, DTF is based on phase difference between EEG signals, so it is hardly influenced by the propagation of electromagnetic field (such propagation does not produce phase differences between EEG derivations; Kaminski and Blinowska, 2014). Bivariate measures of connectivity because of "common feeding" effect often provide a multitude of spurious connections between EEG channels. DTF is free of this effect. Application of pair-wise measures of EEG connectivity leads to finding very dense, close to random patterns, which may outnumber the true connections (Blinowska et al., 2004; Blinowska and Kaminski, 2013).

### 2.5. Classification of Nold and AD individuals by NTDF and COH features

MVAR model of order 5 was fitted to 19 channels of EEG activity used in the present study. In order to get the satisfactory ratio of the number of model parameters to the number of EEG data samples, the ensemble averaging was applied. The correlation matrices calculated in the procedure of model fitting to 2 s EEG segments were averaged over multiple (of the order of 100) segments (Blinowska, 2011). Such procedure effectively increased the number of data points to which the MVAR model was fitted. Then, coherences (ordinary, multiple, partial), NDTF($f$) and ffDTF($f$) estimators were computed, and patterns of propagation were estimated.

For classification procedures, NDTF, ffDTF and coherence (COH) values were integrated into the delta (1–4 Hz), theta (4–8 Hz), alpha (8–13 Hz), beta (13–30 Hz), and gamma (30–45 Hz) bands. In effect, we get matrices (NDTFpairs, ffDTFpairs, and COH) of the dimensions: $19 \times 19 \times 5$ (number of EEG channels $\times$ number of EEG channels $\times$ number of frequency bands) = 1805. They constitute a base for selecting the best features discriminating between Nold and AD subjects. In the discrimination procedure, we considered elements of the above matrices describing relationships between two given EEG channels. Additionally, we added to the battery of parameters, matrices called NDTFsource of dimension $19 \times 5 = 95$. NDTFsource strength was obtained as an average of NDTF values computed between a given electrode and all the remaining ones. NDTFsource quantifies outflows in all directions from a given electrode (source). The choice of this measure of propagation was connected with the fact that some electrodes seem to overlie sources of out propagating EEG activity in practically all directions, and other electrodes only received signals.

As an effect of our computations, we obtained large matrices: NDTFpairs, ffDTFpairs, COH, and NDTFsource, which produced a lot of parameters difficult to be managed for a reliable classification of Nold and AD individuals. Therefore, we reduced the amount of parameters selecting those more effective in the discrimination between the Nold and the AD group. To this aim, the following preliminary exploratory statistical procedure was used:

1. Univariate Student's $t$-tests of all parameters from NDTFpairs, ffDTFpairs, and COH matrices (1,805 comparisons for each matrix) and NDTFsource (95 comparisons) were used to select from the elements (parameters) of the above matrices those showing statistically significant differences between the mean values of the Nold and the AD group. To select NDTFsource parameters showing statistically significant mean differences between the two groups, the customary threshold of $p < 0.05$ two-tailed was used. However, a large number of elements were compared in the case of NDTFpairs, ffDTFpairs, and COH matrices (1,805 comparisons for each matrix), which may generate false positive results. Therefore, the correction for multiple comparisons was done. In the case of 1,805 comparisons, the customary Bonferroni correction would yield significance level of $p < 0.00003$. However, Bonferroni correction assumes independence of the variables to be compared. This is not the case of the EEG variables of the present study. For this reason, the correction for multiple comparisons should be mitigated in respect to Bonferroni procedure (Logan and Rowe, 2004). In this line, we set the significance level at $p < 0.0005$ as a balanced compromise.
2. The parameters selected from NDTFpairs, NDTFsource, ffDTFpairs, and COH matrices by the above statistical analysis were used as an input for the PCA aimed at extracting and integrating main information contents of these parameters (Roy John et al., 1977). For each group of parameters corresponding to NDTFpairs, NDTFsource, ffDTFpairs and COH, we considered only the first principal components accounting for at least 70% of input variance as typically used threshold for this kind of applications (e.g. Lehmann et al., 2007, used 69% threshold). The outcome of this step was the selection of principal components (PCs) representing the extracted main information content of the selected NDTFpairs, NDTFsource, ffDTFpairs, and COH parameters. We called these PCs as "features" for the classification of Nold and AD individuals. For the sake of brevity, we termed these features as NDTFp, NDTFs, ffDTFp, and coh (note that in the following, "COH" is the abbreviation of the matrix of coherence values and "coh" is the abbreviation of the outcome of the principal component analysis upon the COH variables).

For any single Nold or AD subject, NDTFp, NDTFs, ffDTFp, and coh were used as inputs for a computation of the Mahalanobis distance. The procedure to determine the Mahalanobis distance for a given subject was as follows: (i) all subjects (i.e. Nold, AD) were randomly selected and divided into a training group (30 Nold subjects and 30 AD subjects) and a testing group (12 Nold subjects and 12 AD subjects); (ii) for every subject from the testing set, Mahalanobis distances were computed both with respect to the training Nold group and with respect to the training AD group; (iii) the differences between the two Mahalanobis distances (AD minus Nold) were computed as a diagnostic value for every subject indicating tentative AD or Nold classification; (iv) the above procedure was repeated 300 times starting from step (i); (v) classification scores (true positive rate – TPR – and false positive rate – FPR – for each iteration were averaged. These mean classification scores were used as an input to construct ROC curves for the classification of all Nold and AD individuals. This is a standard approach to visualize a balance between TPR and FPR. The index of the goodness of the classification was the area under ROC curve (AUC; Hanley and McNeil, 1982). The ROC curves illustrate the relation between sensitivity and specificity of the classification of Nold and AD individuals. Specifically, ROC is constructed from TPR (= "sensitivity") in the vertical axis and 1–FPR (= "specificity") in the horizontal axis.

## 3. Results

### 3.1. Topographic features of effective (brain) connectivity estimated by EEG rhythms

For illustrative purposes, Fig. 1 shows NDTFpairs values, averaged over subjects and integrated in the frequency range of 1–45 Hz. They represent inter-electrode coupling of the resting state EEG rhythms in the Nold group and in the AD group. In the Nold group, the EEG activity propagates mainly from posterior electrodes (i.e. P3, P4, Pz) towards other electrodes. In comparison to the Nold group, the AD group reveals a similar pattern of NDTFpairs values, but smaller in strength and less dominant in posterior scalp regions.

To better understand these results, we estimated the decrease of the NDTF values as a function of the electrode distance. To this aim, we considered the NDTFsource variable describing the EEG outflow from a given electrode to the other electrodes. The distance, in this case, was not a real topographical distance between electrode pairs, as the distance among the electrodes depends on the head size, which was not measured in the present subjects. The distance was set to 2 for neighboring electrodes of the montage and to $2\sqrt{2}$ for the electrodes lying on the diagonal of the grid for the other electrodes. Fig. 2 shows a decrease of NDTFsource strength with the inter-electrode distance averaged over subjects for two representative electrodes: P4 and T4, for the five EEG frequency bands (i.e. delta, theta, alpha, beta, gamma) and both groups (i.e. Nold, AD). The most pronounced decrease in the NDTFsource strength was observed at the alpha band. The effect was much greater in the Nold group than in the AD group. Other electrodes showed low NDTFsource strength and low decrease of such strength with inter-electrode distance in both groups, regardless the frequency band. These results suggest a reduction in the local connectivity underlying posterior alpha rhythms in the AD group when compared to the Nold group.

### 3.2. Extraction of PCA features for classification from the COH, ffDTFpairs, NDTFpairs, and NDTFsource parameters selected by t-test

The Student's *t*-test selected COH, NDTFpairs, ffDTFpairs, and NDTFsource parameters showing statistical differences between the Nold and the AD group ($p < 0.05$ to 0.0005). These parameters are listed in Supplementary Table S1 and illustrated in Figs. 3–5.

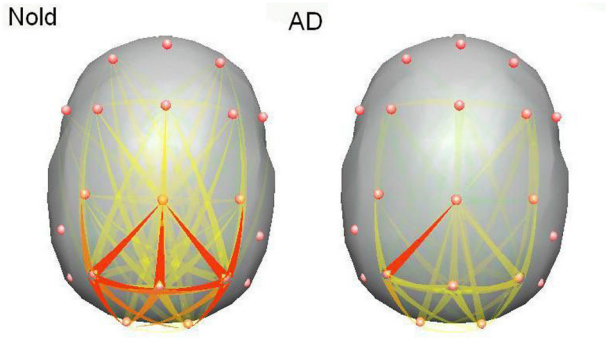


**Fig. 1.** Grand average of non-normalized directed transfer function (NDTF) estimated by resting state eyes-closed EEG in the group of normal elderly subjects (Nold) and the group of Alzheimer's disease (AD) patients. For illustrative purposes, the NDTF estimates refer to a large 0.5–45 Hz frequency band. The magnitude of the NDTF values (arbitrary units) is coded by color (red = the highest NDTF values yellow = the lowest ones) and transparency (low transparency = the highest NDTF values; high transparency = the lowest ones) of the line connecting two electrodes. (For interpretation of the references to color in this figure legend, the reader is referred to the web version of this article.)

They were used as an input to PCA to extract the main information content on the functional (brain) connectivity underlying recorded EEG rhythms. In the majority of cases, first PCs accounted for a remarkable percentage of variance (70%).

Concerning COH, 82 statistically significant values ($p < 0.0005$) were found (see Supplementary Table S1). They referred to the first PC (PC1) and explained desired 70% of the variance. We considered ordinary and partial coherences. Partial coherences are free from "common feeding" effect, they reflect only interactions between two given electrodes, the influences of signals from other electrodes is removed. However, most significant contribution to PC1 was due to ordinary COH in particular, in theta band between frontal/temporal electrodes and between frontal/occipital electrodes. At alpha band, also fronto-frontal ordinary COH values significantly differed between both groups. At beta band, similarly to the higher frequency bands, the main differences between the Nold and the AD group concerned frontal/occipital and frontal/temporal COH values. Compared to the Nold group, the AD group globally showed lower COH values.

For NDTFpairs, 35 statistically significant values ($p < 0.0005$) were found. Most of them referred to the first PC (PC1), the remaining to the second PC (PC2), jointly accounting for 70% of the variance. These significant NDTFpairs values are shown in Fig. 3 together with their PC loadings, which describe a weight of a given parameter in the first principal component. PC loadings provide an information about the importance of particular parameters in the classification procedures. Principal components are constructed as a linear combination of parameters multiplied by the corresponding PC loadings. The NDTFpairs with the highest loadings were observed at alpha band between adjacent posterior electrodes. At higher frequency bands (e.g. beta and gamma), the NDTFpairs with the highest loadings were observed between close electrodes, whereas NDTFpairs with the highest loadings at delta and theta bands were observed not only between close electrodes but also between distant electrodes. Compared to the Nold group, the AD group globally showed lower NDTFpairs values, especially for the direction from posterior electrodes toward neighboring electrodes, also toward distant electrodes.

Concerning ffDTFpairs, only 8 statistically significant values ($p < 0.0005$) were found. They referred to the first PC (PC1), which explained desired 70% of the variance. These significant ffDTFpairs values are shown in Fig. 4 together with their PC loadings, which indicate the importance of a given ffDTFpairs in the classification. The dominant feature for ffDTFpairs was the decrease of its values from P4 to O2 at theta and beta bands for AD group in comparison to Nold group.

Concerning NDTFsource (outflows from a given electrode towards the other electrodes), 30 statistically significant values ($p < 0.05$) referred to the first PC (PC1), which explained desired 70% of the variance. These significant NDTFsource values are shown in Fig. 5 together with their loadings (weights), which indicate the importance of the corresponding parameter in the classification procedures. The NDTFsource showed a decrease from posterior and temporal electrodes mainly at alpha band but also at theta and delta bands. The effect was more pronounced in the AD group in comparison to the Nold group.

For each group of parameters (COH, NDTFpairs, ffDTFpairs, NDTFsource) by means of PCA we have found first components (PC1 s) expressed by a linear combination of significant parameters weighted by the corresponding PC loadings (listed in Supplementary Table S1 and Figs. 3–5). In this way we have reduced the number of variables replacing them by the features (PC1 s) constructed from the optimal combination of parameters.

For illustrative purposes, Fig. 6 shows a representation of all Nold and AD subjects in a multi-dimensional feature space formed by the aforementioned PCs of the selected coh, NDTFp, and NDTFs

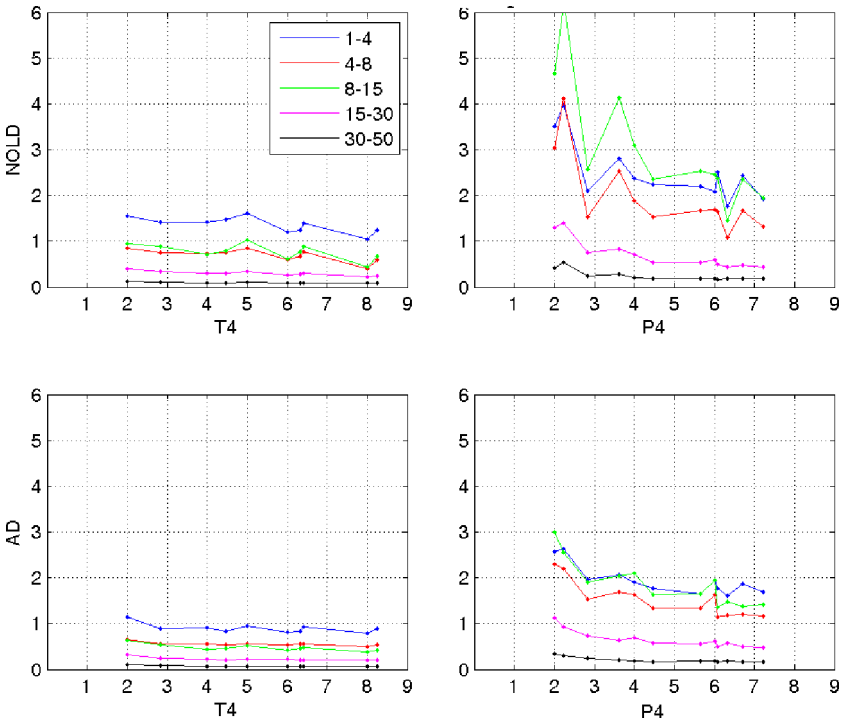


**Fig. 2.** Decrease of NDTF values of EEG rhythms at T4 and P4 electrodes as a function of inter-electrode distance in the Nold and the AD group (averaged over subjects). The inter-electrode distance (horizontal axis) is 2 for the closest neighbors, $2\sqrt{2}$ for electrodes on the diagonal of the grid, etc. The EEG frequency bands of interest depicted in colors are delta (1–4 Hz), theta (4–8 Hz), alpha (8–15 Hz), beta (15–30 Hz), and gamma (30–45 Hz). (For interpretation of the references to color in this figure legend, the reader is referred to the web version of this article.)

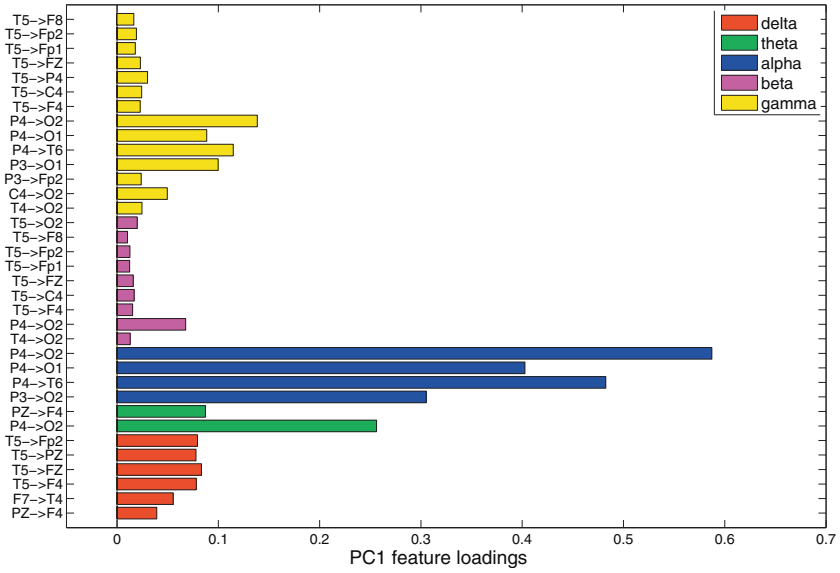


**Fig. 3.** Contribution of NDTFpairs variables to PC1 in terms of PCA loadings. Only these NDTFpairs which showed statistical differences between Nold and AD groups on the level $p < 0.0005$ contributed. The list of electrodes corresponding to these NDTFpairs is marked on the left. For example, the notation "T5- > F8" means directionality of the NDTFpairs values from T5 to F8 electrode. Bars (horizontal axis) show PC loadings of relevant variables. PC loading describes the weight of a given parameter in the principal component. It provides the information about the importance of particular parameter in the classification procedures.

features. It can be observed that these features are able to separate most of the Nold individuals from the AD individuals.

### 3.3. Classification of the Nold and AD individuals

For any single Nold or AD subject, the PCs above called: coh, ffDTFp, NDTFp, and NDTFs features were used as inputs for a procedure computing the Mahalanobis distances from the Nold and the AD group, respectively (see Section 2). We eliminated ffDTF and PC2 of NDTFpairs, since they did not improve the classification of Nold and AD individuals, possibly due to redundancy of information contents in ffDTFpairs and NDTFpairs. The Mahalanobis distances were used as an input to ROC analysis for the classification purposes. The best classification (AUC = 0.85) was obtained when the Mahalanobis distances of the coh, NDTFp, and NDTFs features were taken into account. In order to visualize the

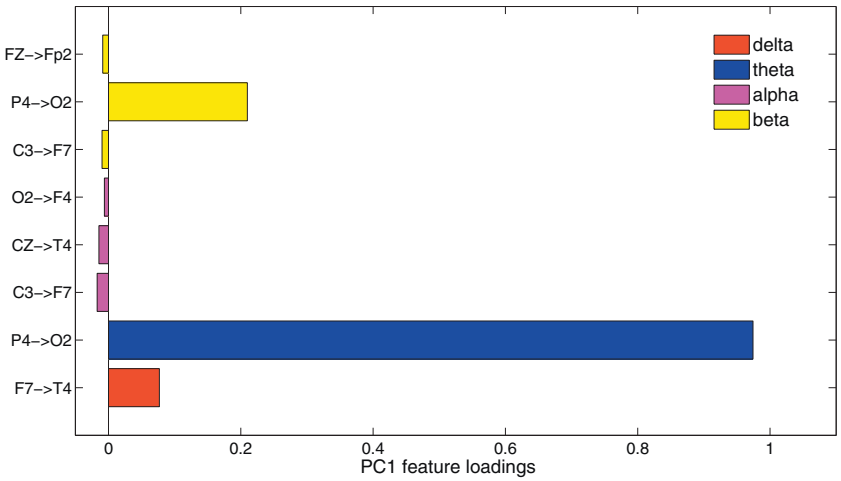


**Fig. 4.** Contribution of ffDTFpairs variables to PC1 in terms of PCA loadings. Only these ffNDTFpairs which showed statistical differences between Nold and AD groups on the level $p < 0.0005$ contributed. The list of electrodes corresponding to these ffDTFpairs is marked on the left. For example, the notation "Fz- > Fp2" means directionality of the ffDTFpairs values from Fz to Fp2 electrode. Bars (horizontal axis) show factor loadings of relevant variables. PC loading describes the weight of a given parameter in the principal component. It provides the information about the importance of particular parameter in the classification procedures.

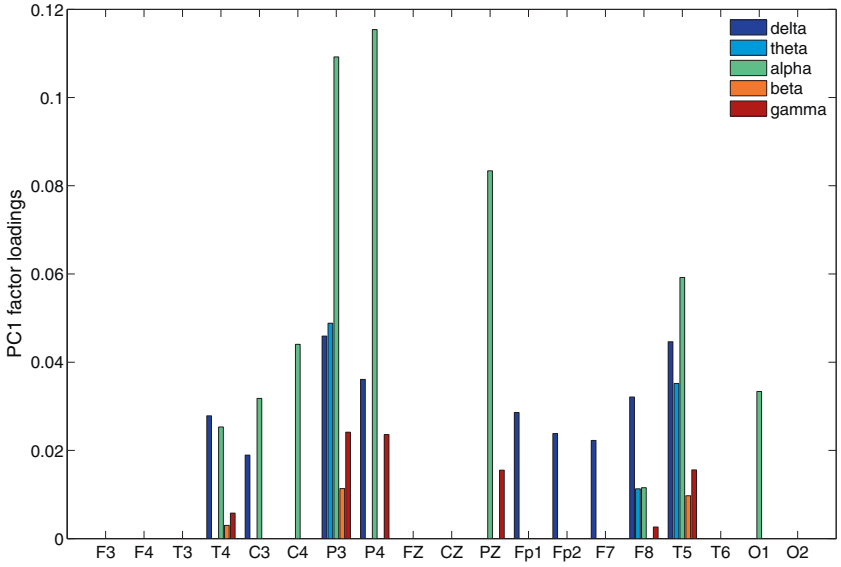


**Fig. 5.** Contribution of NDTFsource variables to PC1 in terms of PCA loadings. NDTFsource variables describe the outflow of activity from a given electrode to all the other electrodes. The source electrodes are marked on the horizontal axis. Bars (vertical axis) show factor loadings of relevant variables. PC loading describes the weight of a given parameter in the principal component. It provides the information about the importance of particular parameter in the classification procedures.

importance of different parameters for the classification, the ROC curves were also constructed for two features only. In this case, the combination of the NDTFp and coh features provided the best classifications (AUC = 0.84). The ROC curves for different combinations of features are shown in Fig. 7A.

As reported above, the Nold and AD groups showed differences in the decay of the NDTFs outflows with the distance between the electrodes (i.e. higher decay in the Nold group than in the AD group (see Fig. 2). Therefore, we defined the following additional discriminating parameters: (i) slopes of the curves describing the decrease of the strengths of total NDTFs outflows at three frequency bands (theta, alpha, beta) and (ii) areas under curves describing the decay of the NDTF with the distance. Such parameters were taken for posterior electrode P3 or P4 (the one with the highest NDTF outflow for a given individual) and were called NDTFs(c). They were added to the battery of the discriminating features. The resulting ROC curves for the combination of NDTFp, coh, and NDTFs(c) features are shown in Fig. 7B.

NDTFs feature did not bring improvement to the classification accuracy any longer, so it was eliminated. The combination of NDTFs(c), NDTFp, and coh improved the classification of the Nold and AD individuals (AUC = 0.86). Fig. 7B plots the ROC curves showing classification rate after elimination of certain features to elucidate the influence of these features on discrimination between Nold and AD individuals. The results of classification expressed in terms of accuracy, precision, sensitivity (TPR) and specificity (1–TPR) are reported in Tables 2 and 3.

In the final step, we added IAF peak values to the battery of discrimination features mentioned above, as an important aspect of dominant alpha rhythms recorded in the resting state eyes-closed condition. The mean IAF peak was statistically lower ($p < 0.01$) in the AD group (8.96 Hz ± 1.3 standard deviation, std)

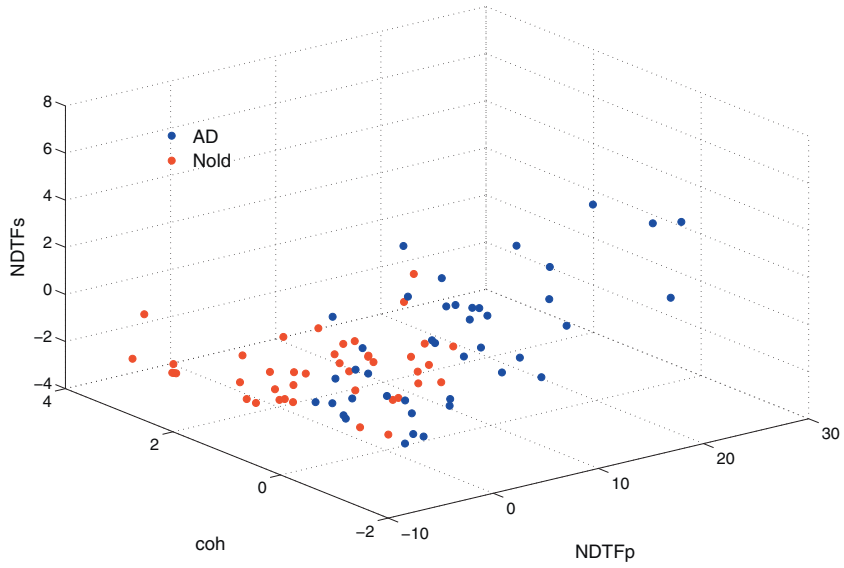


**Fig. 6.** The representation of AD (red circles) and Nold (blue circles) subjects in the space of the following three features: the first components of spectral coherence between electrode pairs (coh), NDTFp and NDTFs. (For interpretation of the references to color in this figure legend, the reader is referred to the web version of this article.)

than in the Nold group (9.74 Hz ± 0.88 std). The inclusion of the IAF peak resulted in an increase of the classification performance (AUC = 0.88; Fig. 7C). In Tables 2 and 3, accuracy, precision, sensitivity, and specificity of the classification between the Nold and AD individuals are reported for the combination of features including NDTFp, NDTFs(c), COH, and IAF peak.

## 4. Discussion

### 4.1. EEG connectivity in AD at the group level

The central hypothesis of this study is that linear estimates of functional (coherences) and effective (NDTF) cortical connectivity computed from resting state eyes-closed EEG time series would characterize AD patients at the group and individual level when compared to Nold subjects. Compared to the Nold group, the AD group showed decreased EEG coherence between posterior and other electrode sites at all frequency bands, with a maximum effect at theta band. The AD group also showed a decrease in the posterior-to-anterior NDTF values, especially at theta (4–8 Hz) and alpha (8–13 Hz) bands. On one hand, this decrease was especially prominent for the long-range NDTF values, especially from parietal regions toward frontal areas. On the other hand, the decay of the NDTF outflow with the inter-electrode distance was greater in the Nold than the AD group. These findings estimating the directional propagation of neural signals from the posterior to anterior cortical areas extend a bulk of previous evidence.

A prominent outflow of EEG activity from posterior electrodes was previously reported in healthy subjects in several frequency bands (Kaminski et al., 1997; Kus et al., 2004). In AD patients, was shown a decreased alpha coherence among temporal-parieto-occipital electrodes, particularly those with a more severe cognitive impairment (Locatelli et al., 1998). Furthermore, there was a reduction in alpha and beta DTF from parietal to frontal electrodes in AD and MCI patients (Babiloni et al., 2008, 2009; Blinowska et al., 2013). These coherence and DTF results were globally cross validated by independent estimates of EEG functional connectivity such as EEG synchronization likelihood (Stam et al., 2003; Babiloni et al., 2004, 2006) and phase lag index (Stam et al., 2009).

The present findings on effective (directional) connectivity complement recent evidence at the source level. (Hsiao et al., 2013) found abnormal source coherence in AD patients in the default mode (i.e. precuneus, posterior cingulate cortex, anterior cingulate cortex and medial temporal regions) and sensorimotor network (Hsiao et al., 2014). In general, the delta and theta source coherence was higher in the AD than in the MCI group in both networks, while the opposite was true for alpha source coherence in the default mode network.

At this early stage of the research, we can just speculate that the prominent effects on posterior (parietal) EEG connectivity in the present study mainly depend on the experimental condition of resting state eyes-closed. This condition is characterized by quiet wakefulness with negligible external stimuli and instructions for no internal substantial mental activity. In this condition, prefrontal cortex (planning and executive control), premotor and somatomotor (somatomotor preparation, execution, and control), temporal (auditory and visual analysis), and occipital (visual analysis) cortical areas are expected to be inhibited, with the exception of their small frontal, parietal, and temporal portions included in the default mode network. When compared to these regions, the parietal cortical area would be less inhibited, due to its role in the continuous processing of somatic information from the body (Pfurtscheller and Lopez da Silva, 1999). This tentative explanation would predict a prominent posterior cortical neural synchronization and an outflow of signals from parietal to other cortical regions in healthy subjects. AD neuropathy involving temporal and parietal regions may affect these neurophysiological mechanisms. As the dominant resting state rhythms are typically observed at theta and alpha frequencies, these rhythms showed maximum changes in AD patients.

### 4.2. EEG connectivity in AD at the individual level

A novel result of the present study was the best classification between the Nold and AD individuals (AUC = 86%) obtained combining the Mahalanobis distances of the first PCs of NDTFp, NDTFs(c), and coherence values. Notably, this classification globally improved (AUC = 88%) by adding IAF peak to the first PCs of NDTFp, NDTFs(c), and coherence values. It is supposed that IAF

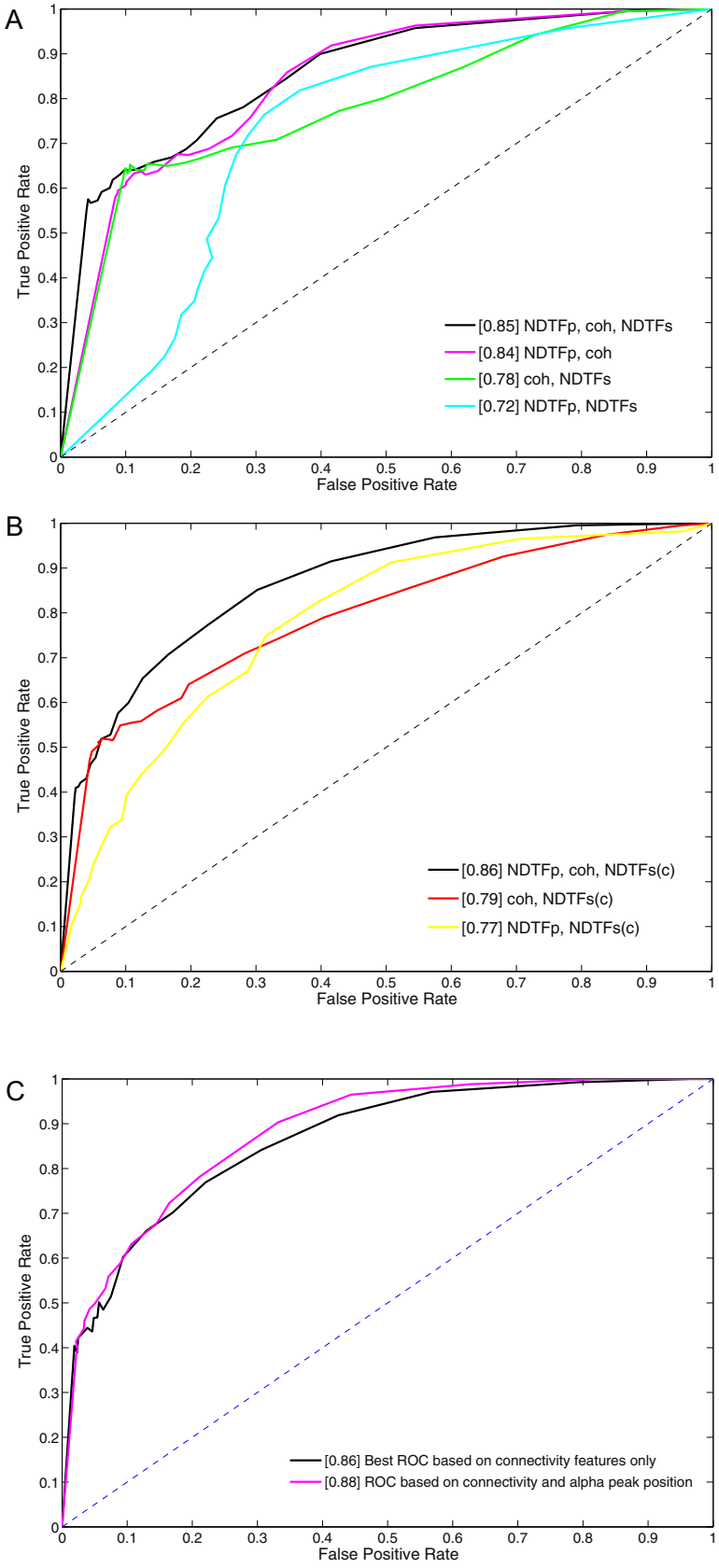


**Fig. 7.** ROC curves for different combinations of the selected features. In the brackets, corresponding values of AUC are given. A- The black curve corresponds to the case when the following features are used for ROC construction. NDTFp (pairs), coh (coherences) and NDTFs (source). Curves marked by different colors correspond to the ROC when only features marked in the insert were used for ROC construction; B – The black curve corresponds to the case when NDTFp, coh and NDTFs(c) features were used for ROC construction. Curves marked by different colors correspond to ROC when only the features listed in the insert were used for ROC construction; C – Black—best ROC curve from Fig. 7B, magenta—ROC curve with alpha peak position added to the connectivity features set (NDTFp, NDTFs(c), coh).

**Table 2**
Results of the classification for the connectivity estimators (NDTFp, NDTFs(c), COH) yielding the best results, expressed in terms of accuracy, precision, sensitivity (TPR) and specificity (1–FPR).

| Accuracy | Precision | Sensitivity (TPR) | Specificity (1–FPR) |
|---|---|---|---|
| 0.7746 | 0.7380 | 0.8514 | 0.6978 |
| 0.7735 | 0.7739 | 0.7728 | 0.7742 |
| 0.7710 | 0.8106 | 0.7072 | 0.8347 |

**Table 3**
Results of the classification for the best connectivity estimators plus alpha peak position, expressed in terms of accuracy, precision, sensitivity (TPR) and specificity (1–FPR).

| Accuracy | Precision | Sensitivity (TPR) | Specificity (1–FPR) |
|---|---|---|---|
| 0.7857 | 0.7314 | 0.9031 | 0.6683 |
| 0.7854 | 0.7610 | 0.8322 | 0.7386 |
| 0.7851 | 0.7875 | 0.7811 | 0.7892 |

peak reflects the frequency slowing of the dominant resting state alpha rhythms due to AD. Indeed, NDTF estimator occurred to be more efficient in classification procedures than ffDTF. Of note, ffDTF reflects a relative flow of signals between electrodes whereas NDTF is proportional to the coupling between electrode pairs (Kaminski et al., 2001). These results point to the global decrease of connectivity in AD. Overall, it can be speculated that the multivariate nature of the present EEG markers explains the above good classification rate. It derives from the auto-regressive model taking into account the correlations among the EEG time series recorded at all electrode pairs of the array. With respect to the present multivariate estimators, bivariate EEG estimators may provide an appraisal of spurious connections due to the "common feeding" effect (Blinowska et al., 2004; Kus et al., 2004). From a formal point of view, for bivariate (i.e. pair-wise) measures such as e.g.: FFT computation of between-electrode coherence, $N$ true connections and $N(N-1)/2$ false connections may be created, respectively (Blinowska and Kaminski, 2013). Therefore, when bivariate measures are applied, the number of false connections increases as $N^2$ with the number of electrodes recording EEG activity from a given cortical source, whereas true connections increase only as $N$ (Blinowska and Kaminski, 2013). Another beneficial feature of the present EEG markers, especially DTF, is a fact that it is hardly influenced by volume conduction (Kaminski and Blinowska, 2014).

A comparison of the present classification results with those of previous EEG studies in the AD field is difficult, due to the plurality of the methodological approaches and the variables used in the past. In some studies, voltages of resting state eyes-closed EEG rhythms were used as an input to artificial neural networks (ANNs; Buscema et al., 2007; Rossini et al., 2008). In other studies, EEG power density, coherence, and markers based on the chaos theory served as inputs to linear and non-linear classifiers in mild to moderate AD (Anderer et al., 1994; Pritchard et al., 1994; Nuwer, 1997; Huang et al., 2000; Bennys et al., 2001; Buscema et al., 2007; Lehmann et al., 2007). More specifically, Pritchard et al. (1994) used Mahalanobis distance and leave-one-out discrimination procedure, reaching a sensitivity of 71.5% and a specificity of 80%. When they applied an ANN as a classifier, the discrimination improved to a sensitivity of 85.7% and specificity of 96%. Furthermore, Anderer et al. (1994) used spectral EEG variables as an input to an ANN. Results showed a sensitivity of 90% and specificity of 75% in the classification of Nold and dementia individuals. For the same purpose, Lehmann et al. (2007) used EEG power density and coherence in ANN and "random forest" classification procedures. Results showed a sensitivity of 85% and a specificity of 78% by the "random forest" classification, as well as a sensitivity of 89% and a specificity of 88% by ANN. More recently, Dauwels et al. (2010b) have tested more than 30 EEG variables of linear and nonlinear functional and effective (brain) connectivity. Results showed that only two estimators yielded statistically significant sensitivity in the classification between Nold and MCI individuals, namely SES (68% of sensitivity) and ffDTF (70% of sensitivity). The combination of these parameters yielded sensitivity of 83% (Dauwels et al., 2010b).

What about the comparison in the classification accuracy between the markers of EEG connectivity and those based on CSF, MRI, and PET? Results based on CFS study yielded discrimination sensitivity (SEN) in the range: 70–100% and 40–85% for amyloid β and tau respectively, corresponding specificities (SPE) were 40–85% and 65–85% (Sunderland et al., 2003; Beach et al., 2012). Ratio tau/amyloid β yielded higher values, up to SEN 95% and SPE 80% (Fagan et al., 2011). Overall, ranges of classification accuracy are in the same order of magnitude as those of the EEG markers, motivating more efforts toward an integration of EEG connectivity and the other markers in future studies.

### 4.3. Limitations and perspectives of the present methodological approach

The present results are quite promising, but their clinical neurophysiological interpretation should take into account some methodological limitations. As mentioned in the Methods (Subjects), the current exploratory study is based on small groups of AD and Nold individuals reflecting the typical epidemiological characteristics of AD population, namely the AD patients were typically older and less educated than the Nold subjects were. Therefore, the interpretation of the results should take into account this slight but significant difference (independent $t$-test, $p < 0.05$) in the demographic variables of the two groups. We cannot exclude that the small but important differences in those variables affected the present classification accuracy even if it is entirely improbable that this possible effect changes the evidence of a moderate discrimination of AD individual around 80%.

Another limitation of the present study is that the AD patients were treated with acetylcholinesterase inhibitors. Furthermore, a minority of them use anxiolytic agents. A partial mitigation of this confound is that previous findings predict that long-term Acetylcholinesterase inhibitors exert an effect of neuroprotection on the EEG activity revealed by EEG markers, thus suggesting that the classification accuracy between Nold and AD individuals would have been better with AD patients not taking any long-term treatment with Acetylcholinesterase inhibitors (Babiloni et al., 2006). Furthermore, anxiolytic (e.g. benzodiazepine) mainly affect the high frequency of resting state EEG activity (beta band; Laurijssens and Greenblatt, 1996) which plays secondary role in the discrimination between Nold and AD individuals. The present results should be cross-validated in de novo AD patients free from any psychoactive medication.

Another methodological limitation is the analysis of functional and effective EEG connectivity at only 19 scalp electrodes rather than cortical level. Functional EEG connectivity computed at EEG electrodes might not reveal a direct neuroanatomical connection between the cortical regions underlying the scalp ones where EEG signal is recorded. As mentioned in the Introduction, this intrinsic confound of scalp EEG techniques is due to residual effects of head volume conduction of neural currents and "common feeding" of EEG signals coming from remote cortical or sub-cortical regions. The present methodological approach mitigates this general limitation. Effective connectivity measures used in this study – NDTF and ffDTF – are free from "common feeding" effect. Furthermore, they are much less influenced from head volume con-

duction than ordinary coherences computed from EEG signals recorded at scalp regions are (Kaminski and Blinowska, 2014).

Concerning the use of high EEG spatial sampling (e.g. 64–128 electrodes) and cortical source estimation techniques, is reasonable that they might potentially improve the spatial resolution in the modeling of cortical functional connectivity from scalp EEG data. However, they need more methodological research before clinical application. Indeed, presently the impact of a different impedance across scalp electrodes on cortical source estimation from high-resolution montages is unclear (AD patients typically ask to speed the montage of 64–128 electrodes, practically not allowing an accurate lowering of the electrode impedance). Furthermore, cortical source estimation can affect the phases of EEG rhythms and, then, the validity of the computation of functional and effective connectivity based on the comparison of these phases in different areas. For this reason, at this early stage of the research we opted for the use of a safe, traditional clinical procedure of EEG spatial sampling (i.e. 19 electrodes) and the analysis of the EEG connectivity at scalp level.

In our opinion, two lines of future studies may exploit the use of the present approach. In the first research line, PCA, Mahalanobis distance, and ROC analysis may be used to extract and integrate main information contents not only from the present multivariate coherence and DTF markers but also from other markers derived from information theory, synchronization and phase difference (Sakkalis, 2011). However, it should be noted that bivariate EEG markers are often affected by spurious false positive solutions due to "common feeding", so the effective contribution of them to the classification purpose should be preliminary tested. Additionally, most of these measures (except the ones based on phase difference) are influenced by volume conduction of electromagnetic fields. Again, this should be taken into account by preliminary tests on simulated EEG data. In the second research line, functional and effective connectivity measures followed by PCA may be associated to smart linear and nonlinear classifiers previously used for the successful classification of Nold and AD individuals such as discriminant analysis, random forest, support vector machine, and ANNs (Anderer et al., 1994; Pritchard et al., 1994; Lehmann et al., 2007).

The future prospective studies concerning the cross-validation of the results may also concern MRI markers of diffusion tensor imaging (DTI) available in the same Nold and AD subjects enrolled for the continuation of EEG studies. These MRI markers provide a measurement of the integrity of bundle of white matter connecting cortical regions of interest. It is expected that abnormal functional connectivity of EEG rhythms in AD patients be correlated with alterations of DTI in corresponding white matter bundles (references on DTI-MRI and EEG-connectivity in AD patients). Finally, cross-validation protocol of future studies should include more than one large independent databases of EEG data in Nold and AD subjects to test the replicability of the results.

## 5. Conclusions

The present exploratory study used multivariate EEG markers of functional and effective connectivity for the classification of Nold and AD individuals (Blinowska and Kaminski, 2013). The PCA and Mahalanobis distance combined and integrated these EEG markers while AUC provided the goodness of discrimination. Compared to the Nold group, the AD group showed decreased coherence estimates, especially in posterior and temporal regions at theta band. Furthermore, there was a decrease in the posterior-to-anterior NDTF estimates, especially at theta (4–8 Hz) and alpha (8–13 Hz) bands. The best classification of the Nold and AD individuals was obtained combining and integrating the most relevant EEG markers derived from coherence and NDTF values (AUC = 0.86%). Furthermore, this classification further improved by adding the IAF peak as an index of global brain synchronization at alpha frequencies (AUC = 0.88%). The results of the present study suggest that combining and integrating linear EEG estimates of brain connectivity (coherence, NDTF) and synchronization (IAF) provide a good classification of Nold and AD individuals around 80%, even considering the methodological limitations in the composition of the Nold and AD groups (i.e. slight but significant differences in the demographic variables of the Nold and AD groups in the present exploratory study, use of Acetylcholinesterase inhibitors, etc.).

These encouraging results motivate a cross-validation study of the new procedure in age- and education-matched Nold, stable and progressing mild cognitive impairment individuals and de novo AD patients with dementia. If cross-validated, the new procedure will provide cheap, broadly available, repeatable over time, and entirely non-invasive EEG topographic markers reflecting abnormal cortical connectivity in AD patients diagnosed by direct or indirect measurement of cerebral amyloid β and hyperphosphorylated tau peptides. More specifically, it is expected that the multivariate markers of EEG connectivity may enrich the instrumental assessment of AD patients with dementia or MCI, diagnosed on the basis of pathophysiological CSF and PET markers of AD in line with the recent international guidelines of (Dubois et al., 2014).

## Acknowledgments

The present study was supported by the Polish Ministry of Science and Higher Education (Decision no. 1682/7. PR UE/2010/7). Furthermore, it was developed in the framework of the following projects"Smart Health 2.0" (Italian Ministry of University and Technological Research, Pon04a2_C-MIUR D.D. 626/Ric e 703/Ric), "CONNAGE" (Italian Ministry of University and Technological Research, PRIN2010-2011, prot. 2010SH7H3F), "Diagnostic Enhancement of Confidence by an International Distributed Environment" (DECIDE; FP7 ICT "infrastructure" 2010-2012; www.eu-decide.eu) and Statutory Grant of Polish Ministry of Science and Higher Education to Faculty of Physics of University of Warsaw (MK) and Nalecz Institute of Biocybernetics and Biomedical Engineering (KB).

*Conflict of interest statement:* None of the authors have potential conflicts of interest to be disclosed. All funding sources are mentioned in the Acknowledgements section, and none of the sponsors had any involvement in the collection, analysis, and interpretation of data, nor in the writing of the manuscript.

## Appendix A. Supplementary data

Supplementary data associated with this article can be found, in the online version, at http://dx.doi.org/10.1016/j.clinph.2016.10.002.

## References

Anderer P, Saletu B, Kloppel B, Semlitsch HV, Werner H. Discrimination between demented patients and normals based on topographic EEG slow wave activity: comparison between z statistics, discriminant analysis and artificial neural network classifiers. Electroencephalogr Clin Neurophysiol 1994;91:108–17.

Babiloni C, Ferri R, Moretti DV, Strambi A, Binetti G, Dal Forno G, Ferreri F, Lanuzza B, Bonato C, Nobili F, Rodriguez G, Salinari S, Passero S, Rocchi R, Stam CJ, Rossini PM. Abnormal fronto-parietal coupling of brain rhythms in mild Alzheimer's disease: a multicentric EEG study. Eur J Neurosci 2004;19(9):2583–90.

Babiloni C, Ferri R, Moretti DV, Binetti G, Cassarino A., Dal Forno G, Ercolani M., Ferreri, Frisoni F, F, Lanuzza B, Miniussi C., Nobili F, Rodriguez G, Rundo F., R, Stam C J, Muscha T., Vecchio F, Rossini PM. Fronto-parietal coupling of brain rhythms in mild cognitive impairment: a multicentric EEG study. Brain Res Bull 2006;69:63–73.

Babiloni C, Frisoni GB, Pievani M, Vecchio F, Infarinato F, Geroldi C, Salinari S, Ferri R, Fracassi C, Eusebi F, Rossini PM. White matter vascular lesions are related to

parietal-to-frontal coupling of EEG rhythms in mild cognitive impairment. Hum Brain Mapp 2008;29(12):1355–67.
Babiloni C, Ferri R, Binetti G, Vecchio F, Frisoni GB, Lanuzza B, Miniussi C, Nobili F, Rodriguez G, Rundo F, Cassarino A, Infarinato F, Cassetta E, Salinari S, Eusebi F, Rossini PM. Directionality of EEG synchronization in Alzheimer's disease subjects. Neurobiol Aging 2009a;30(1):93–102.
Babiloni C, Frisoni G, Vecchio F, Lizio R, Pievani M, Geroldi C, Fracassi C, Vernieri F, Ursini F, Rodriguez G, Nobili F, Salinari S, Van Dijkman S, Ferri R, Rossini PM. Global functional coupling of resting EEG rhythms is abnormal in mild cognitive impairment and Alzheimer's Disease. A multicenter EEG study. J Psychophysiol 2009b;23(4):224–34.
Babiloni C, Lizio R, Del Percio C, Marzano N, Soricelli A, Salvatore E, Ferri R, Cosentino Fi, Tedeschi G, Montella P, Marino S, De Salvo S, Rodriguez G, Nobili F, Vernieri F, Ursini F, Mundi C, Richardson Jc, Frisoni Gb, Rossini Pm. Cortical sources of resting state eeg rhythms are sensitive to the progression of early stage Alzheimer's Disease. J Alzheimer's Dis 2013;34(4):1015-35.
Babiloni C, Lizio R, Marzano N, Capotosto P, Soricelli A, Triggiani AI, Cordone S, Gesualdo L, Del Percio C. Brain neural synchronization and functional coupling in Alzheimer's disease as revealed by resting state EEG rhythms. Int J Psychophysiol 2015. pii: S0167-8760(15)00038-0.
Beach TG, Monsell S, Phillips LE, Kukull W. Accuracy of the Clinical Diagnosis of Alzheimer Disease at National Institute on Aging Alzheimer's Disease Centers, 2005–2010. J Neuropath Exp Neurol 2012;71(4):266–73.
Bennys K, Rondouin G, Vergnes C, Touchon J. Diagnostic value of quantitative EEG in Alzheimer disease. Neurophysiol Clin 2001;31:153–60.
Blinowska KJ, Kuś R, Kamiński M. Granger causality and information flow in multivariate processes. Phys Rev E 2004;70:050902.
Blinowska K J, Kaminski M. Multivariate Signal Analysis by Parametric Models. In: Schelter B, Winterhalder M, Timmer J, editors. Handbook of Time Series Analysis. Wiley-VCH Verlag; 2006. p. 387–420.
Blinowska KJ. Review of the methods of determination of directed connectivity from multichannel data. Med Biol Eng Comput 2011;49:521–9.
Blinowska KJ, Zygierewicz J. Practical Biomedical Signal Analysis Using Matlab. Boca Raton, London, New York: CRC Press; 2012.
Blinowska K, De Vico Fallani F, Lizio R, Vecchio F, Rakowski F, Kaminski M, Lesyng B, Babiloni C. Functional connectivity in Alzheimer's disease and Mild Cognitive Impairment: an EEG study in the framework of DECIDE project. Proc. BIOMAG2012, Paris, 26-30, August 2012.
Blinowska KJ, Kaminski M. Functional Brain Networks: Random, "Small World" or Deterministic? PLoS ONE 2013;8(10):e78763.
Braak H, Rub U, Schultz C, Del Tredici K. Vulnerability of cortical neurons to Alzheimer's and Parkinson's diseases. In: Perry G, Avila J, Kinoshita J, Smith MA, editors. Alzheimer's disease: a century of scientific and clinical research. Amsterdam: IOS Press; 2006. p. 35–44.
Buscema M, Rossini P, Babiloni C, Grossi E. The IFAST model, a novel parallel nonlinear EEG analysis technique, distinguishes mild cognitive impairment and Alzheimer's disease patients with high degree of accuracy. Artif. Intell. Med. 2007;40(2):127–41.
Claus JJ, Strijers RL, Jonkman EJ, Ongerboer de Visser BW, Jonker C, Walstra GJ, Scheltens P, Van Gool WA. The diagnostic value of electroencephalography in mild senile Alzheimer's disease. Clin Neurophysiol 1999;110:825–32.
Dauwels J, Vialatte F, Cichocki A. Diagnosis of Alzheimer's Disease from EEG Signals: Where Are We Standing? Curr Alzheimer Res 2010a;7(6):487–505.
Dauwels J, Vialatte F, Musha T, Cichocki A. A comparative study of synchrony measures for the early diagnosis of Alzheimer's disease based on EEG. Neuroimage 2010b;49(20):668–93.
Delbeuck X, Van der Linden M, Collette F. Alzheimer's disease as a disconnection syndrome? Neuropsychol Rev 2003;13:79–92.
Dubois B, Feldman HH, Jacova C, Hampel H, Molinuevo JL, Blennow K, DeKosky ST, Gauthier S, Selkoe D, Bateman R, Cappa S, Crutch S, Engelborghs S, Frisoni GB, Fox NC, Galasko D, Habert MO, Jicha GA, Nordberg A, Pasquier F, Rabinovici G, Robert P, Rowe C, Salloway S, Sarazin M, Epelbaum S, de Souza LC, Vellas B, Visser PJ, Schneider L, Stern Y, Scheltens P, Cummings JL. Advancing research diagnostic criteria for Alzheimer's disease: the IWG_ criteria. Lancet Neurol 2014;13(6):614–29.
Fagan M, Shaw LM, Xiong C, Vanderstichele H, Mintun MA, Trojanowski JQ, Coart E, Morris JC, Holtzman DM. Comparison of analytical platforms for cerebrospinal fluid measures of β-Amyloid 1–42, total tau, and P-tau181 for identifying Alzheimer disease amyloid plaque pathology. JAMA Neurol 2011;68 (9):1137–44.
Folstein MF, Folstein SE, McHugh PR. 'Mini Mental State' a practical method for grading the cognitive state of patients for clinician. J Psychiatr Res 1975;12:189–98.
Friston KJ. Functional and effective connectivity: a review. Brain Connectivity 2011;1(1):13–36.
Gallego-Jutgla E, Sole-Casals J, Vialatte F-B, Elgendi M, Cichocki A, Dauwels J. A hybrid feature selection approach for the early diagnosis of Alzheimer disease. J Neural Eng 2015;12(1):016018.
Granger CWJ. Investigating causal relations in by econometric models and cross-spectral methods. Econometrica 1967;37. 424-348.
Hanley JA, McNeil BJ. The meaning and use of the area under a receiver operating characteristic (ROC) curve. Radiology 1982;143(1):29–36.
Hsiao F, Chen W, Wang Y, Yan S, Lin Y. Altered source-based EEG coherence of resting-state sensorimotor network in early-stage Alzheimer's disease compared to mild cognitive impairment. Neurosci Lett 2014;558:47–52.
Hsiao F, Wang Y, Yan S, Chen W, Lin Y. Altered oscillation and synchronization of default-mode network activity in mild Alzheimer's disease compared to mild cognitive impairment: an electrophysiological study. PLoS ONE 2013;8(7): e68792.
Huang C, Wahlund L, Dierks T, Julin P, Winblad B, Jelic V. Discrimination of Alzheimer's disease and mild cognitive impairment by equivalent EEG sources: a cross-sectional and longitudinal study. Clin Neurophysiol 2000;111:1961–7.
Hughes CP, Berg L, Danziger WL, Cohen LA, Martin RL. A new clinical rating scale for the staging of dementia. Br J Psychiatry 1982;140:1225–30.
Jeong J. EEG dynamics in patients with Alzheimer's disease. Clin Neurophysiol 2004;115:1490–505.
Jackson CE, Snyder PJ. Electroencephalography and event-related potentials as biomarkers of mild cognitive impairment and mild Alzheimer's disease. Alzheimer's Dement 2008;4:137–43.
Kaminski M, Blinowska KJ. A new method of the description of the information flow in brain structures. Biol Cybern 1991;65:203–10.
Kaminski M, Blinowska KJ, Szelenberger W. Topographic analysis of coherence and propagation of EEG activity during sleep and wakefulness. Electroencephalogr Clin Neurophysiol 1997;102:216–27.
Kaminski M, Blinowska KJ. Directed transfer function is not influenced by volume conduction—inexpedient pre-processing should be avoided. Front Comput Neurosci 2014;8:61.
Kaminski M, Ding M, Truccolo W, Bressler S. Evaluating causal relations in neural systems: Granger causality, directed transfer function and statistical assessment of significance. Biol Cybern 2001;85:145–57.
Klimesch W. EEG alpha and theta oscillations reflect cognitive and memory performance: a review and analysis. Brain Res 1999;29:169–95.
Kus R, Kamiński M, Blinowska KJ. Determination of EEG activity propagation: pair-wise versus multichannel estimate. IEEE Trans Biomed Eng 2004;51:1501–10.
Laurijssens BE, Greenblatt DJ. Pharmacokinetic-pharmacodynamic relationships for benzodiazepines. Clin Pharmacokinet 1996;30:52–76.
Lawton MP, Brodie EM. Assessment of older people: self maintaining and instrumental activity of daily living. J Gerontol 1969;9:179–86.
Lehmann C, Koenig T, Jelic V, Prichep L, John RE, Wahlund LO, Dodge Y, Dierks T. Application and comparison of classification algorithms for recognition of Alzheimer's disease in electrical brain activity (EEG). J Neurosci Methods 2007;161:342–50.
Locatelli T, Cursi M, Liberati D, Franceschi M, Comi G. EEG coherence in Alzheimer's disease. Electroencephalogr Clin Neurophysiol 1998;106:229–37.
Logan BR, Rowe DB. An evaluation of thresholding techniques in fMRI analysis. Neuroimage 2004;22:95–108.
Lund and Manchester Groups. Clinical and Neuropathological criteria for frontotemporal dementia. J Neurol Neurosurg Psychiatry 1994;57:416–8.
McKhann G, Drachman D, Folstein M, Katzman R, Price D, Stadlan EM. Clinical diagnosis of Alzheimer's disease: report of the NINCDS-ADRDA Work Group under the auspices of Department of Health and Human Services Task Force on Alzheimer's disease. Neurology 1984;34:939–44.
Novelli G, Papagno C, Capitani E, Laiacona M, Vallar G, Cappa SF. Tre test clinici di ricerca e produzione lessicale. Taratura su soggetti normali. Archivio di Psicologia, Neurologia e Psichiatria 1986;47:477–506.
Nuwer M. Assessment of digital EEG, quantitative EEG, and EEG brain mapping: report of the American Academy of Neurology and the American Clinical Neurophysiology Society. Neurology 1997;49:277–92.
Pfurtscheller G, Lopez da Silva F. Event-related EEG/MEG synchronization and desynchronization: basic principles. Clin Neurophysiol 1999;110:1842–57.
Pievani M, Haan W, Wu T, Seeley WW, Frisoni GB. Functional network disruption in the degenerative dementias. Lancet Neurol 2011;10(9):829–43.
Pritchard WS, Duke DW, Coburn KL, Moore NC, Tucker KA, Jann MW, et al. EEG-based, neural-net predictive classification of Alzheimer's disease versus control subjects is augmented by non-linear EEG measures. Electroencephalogr Clin Neurophysiol 1994;91:118–30.
Reitan RM. Validity of the Trail Making Test as an indicator of organic brain damage. Percept Mot Skills 1958;8:271–6.
Rey A. Reattivo della figura complessa. Firenze: Organizzazioni Speciali; 1968.
Roman GC, Tatemichi TK, Erkinjuntti T, Cummings JL, Masdeu JC, Garcia JH, Amaducci L, Orgogozo JM, Brun A, Hofman A, et al. Vascular dementia: diagnostic criteria for research studies. Report of the NINDS-AIREN International Workshop. Neurology 1993;43(2):250–60.
Rosen WG, Terry RD, Fuld PA, Katzman R, Peck A. Pathological verification of ischemic score in differentiation of dementias. Ann Neurol 1980;7(5):486–8.
Rossini PM, Rossi S, Babiloni C, Polich J. Clinical neurophysiology of aging brain: from normal aging to neurodegeneration. Prog Neurobiol 2007;83 (6):375–400.
Rossini PM, Buscema M, Capriotti M, Grossi E, Rodriguez G, Del Percio C, Babiloni C. Is it possible to automatically distinguish resting EEG data of normal elderly vs. mild cognitive impairment subjects with high degree of accuracy? Clin Neurophysiol 2008;119(7):1534–45.
Roy John E, Karmel B, Corning WC, Easton P, Brown D, Ahn H, John M, Harmony T, Prichep L, Toro A, Gerson I, Bartlet F, Thatcher R, Kaye H, Valdes P, Schwartz E. Neurometrics. Science 1977;196:1393–410.
Sakkalis V. Review of advanced techniques for the estimation of brain connectivity measured with EEG/MEG. Comput Biol Med 2011;41(12):1110–7.
Spinnler H, Tognoni G. Standardizzazione e taratura italiana di test neuropsicologici. Ital J Neurol Sci 1987;8(Suppl.):1–120.

Stam CJ, van der Made Y, Pijnenburg YAL, Scheltens PH. Synchronization of brain activity in mild cognitive impairment and early Alzheimer's disease. Acta Neurol Scand 2003;108:90–6.

Stam CJ, de Haan W, Daffertshofer A, Jones BF, Manshanden I, van Cappellen van Wlsum AM, Montez T, Verbunt JPA, Munck JC, Van Dijk BW, Berendse HW, Scheltens P. Graph theoretical analysis of magnetoencephalographic functional connectivity in Alzheimer's disease. Brain 2009;132:213–24.

Sunderland T, Linker G, Nadeem Mirza N, Putnam KT, Friedman DL, Kimmel LH, Bergeson J, Manetti GJ, Zimmermann M, Tang B, Bartko JJ, Cohen RM. Decreased â-Amyloid1-42 and Increased Tau Levels in Cerebrospinal Fluid of Patients with Alzheimer Disease. JAMA 2003;289:2094–103.

Terry A, Buccafusco J. The cholinergic hypothesis of age and Alzheimer's disease-related cognitive deficits: recent challenges and their implications for novel drug development. J Pharmacol Exp Ther 2003;306:821–7.

Yesavage JA, Brink TL, Rose TL, Lum O, Huang V, Adey M, Leirer VO. Development and validation of a geriatric depression screening scale: a preliminary report. J Psychiatr Res 1982-83;17:37–49.